BACKGROUND PAPER

Prepared for the 2015 Global Assessment Report on Disaster Risk Reduction

ASSESSING THE AGRICULTURAL DROUGHT RISKS FOR PRINCIPAL RAINFED CROPS DUE TO CHANGING CLIMATE SCENARIOS USING SATELLITE ESTIMATED RAINFALL IN AFRICA

Harikishan Jayanthi

2014

Assessing the agricultural drought risks for principal rainfed crops due to changing climate scenario using satellite estimated rainfall in Africa

1. Introduction

Human-induced climate-change is modifying the established terrestrial and regional weather patterns. This is leading to unexpected cultural, economic, environmental, and social changes in most of the under- and developing countries. Although scientific programs and technologies are available to monitor and forecast the weather and climate extremes at different scales there are however very few methods available to model the consequent impacts on various sectors of society. In the context of hydro-meteorological extremes, droughts and floods are most projected natural disasters to increase in frequency and intensity. IFPRI (2013) stated that agriculture accounts for more than 50 percent of GDP in Burundi, DRC, Ethiopia, Sudan and Tanzania, while it accounts for less than 30 percent of GDP in Eritrea, Kenya and Madagascar. Increased frequency of droughts and floods in these countries would not only disturb the primary economy-driver but also disrupt the value chain linking the secondary and tertiary sectors with agriculture.

Floods are characterized by periods where above-normal rainfall cause overland and riverine inundations. Their times of onset and ending are distinct; whose affected areas are well defined (flood plains); and whose hazard is measured in terms of depth of inundation and/or above-normal discharges. On the other hand drought is considered as a creeping phenomenon whose starting point is indistinct; it spread varying in terms of weeks to decades depending on the hydro-climatic characteristics of the region. Drought impact depends on the inter-dependence between the rainfall, its deviation from normal, and the demands of the agencies for survival (http://drought.unl.edu/DroughtBasics/WhatisDrought.aspx). In the context of agriculture, droughts cause physiological (than physical) damage to crops and this further complicates the assessment mechanism as crops have non-linear response to water deficit; and possess a certain degree of resilience to water deficits. In the context of agricultural drought risk assessment, it becomes very important to first understand the conceptualization of drought before establishing mechanisms for modeling its risks in agriculture.

2. Conceptualizations of drought

UNISDR (2009) defined drought as a precipitation-deficiency over an extended period of time (one growing season or longer) causing critical shortages for water-dependent activities, groups, and environmental sectors. That report highlighted that the droughts are temporary natural aberrations whose characteristics vary significantly from region to region and are different from climatic features like aridity observed in perpetually low rainfall regions of the world. Wilhite and Glantz (1985) analyzed more than 150 definitions all over the world and grouped them into 4 major categories, namely meteorological, agricultural, hydrological and socio-economic droughts, and figure 1 summarizes their inter-relationships.
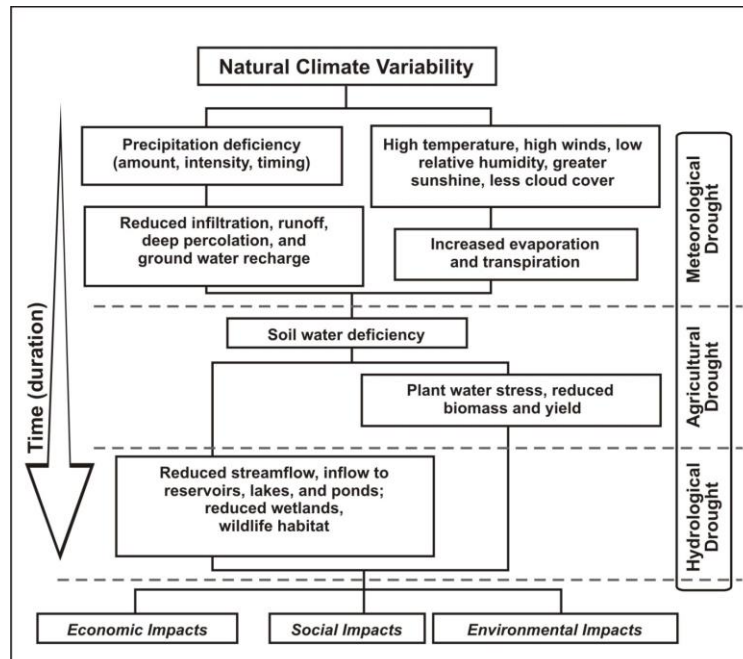
Fig. 1 Drought typologies and the cascading impact relationships (Source: National Drought Mitigation Center, University of Nebraska-Lincoln, USA (http://www.drought.unl.edu/DroughtBasics/TypesofDrought.aspx)

Sivakumar et al. (2011) observed that although many meteorological indices of agricultural droughts are available and often used, they are less than ideal because pertinent physical and biological factors are not built in to them. It was recommended, rather, that an agricultural drought index should integrate precipitation and temperature, along with evapotranspiration (ET) and soil moisture deficits for effective monitoring of agricultural droughts affecting rainfed crops, pasture, and rangeland. Note that irrigated agriculture can suffer production shortfalls due to water shortages stemming from inadequate stream flow, ground water pumpage, and/or reservoir storage.

With regard to planning, Wilhite (1991) published a 10-step generic process for developing drought risk management plans and capacity building activities in drought prone countries of the world. Monnik (2000) proposed a drought early warning system (DEWS) that would provide the decision maker with objective information on the onset, continuation, and termination of drought conditions with the following data: (1) meteorology, (2) crop area and production, (3) food and forage prices, (4) drinking water, and (5) household vulnerability data in near real time.

Wilhite and Svoboda (2000) reviewed the state-of-the-practice summarizing the DEWS in Brazil, Hungary, India, Nigeria, South Africa, and the United States. They highlighted the then prevailing systemic and methodological inadequacies, namely the lack of a well-defined common drought index (or indices), inadequate density and data quality of hydro-meteorological parameters, restrictions regarding timely data sharing,

non-user-friendly information products, incomplete and piecewise analyses of the drought phenomenon, lack of clear drought impact assessment methodology, unreliable drought forecasting, inadequate dissemination systems, and lack of a global drought assessment system in the world. Since then progress has been made, for example, with the National Integrated Drought Information System (NIDIS) in the U.S., which has piloted sub-national drought early warning systems in several important river basins (www.drought.gov). On a related note, the GAR (2011) highlighted the continuing absence of a credible drought risk mechanism, which was attributed to various hydro-meteorological observational challenges as well as the socio-economic drivers such as poverty and rural vulnerability, industrialization and urbanization, and weak and ineffective governance.

3.   Drought risk management

UNDP (2011) identified 5 basic steps in the mainstreaming philosophy of drought risk management (DRM): (1) identify stakeholders and establish a coordination mechanism, (2) assess hazard trends and vulnerabilities (the basis for a drought risk database and drought risk profiles), (3) identify mitigation measures and evaluate where these will be integrated, (4) incorporate the measures in the development of policy and planning, and (5) monitor and evaluate the impacts of the entire mechanism. The backbone of the entire DRM philosophy hinges on the accuracy of the drought profiling in a given area, essentially consisting of analyzing long term climate records, understanding the changes in the seasonal distribution of weather parameters, land use/land cover changes, crop practices, and hydrologic records. A functioning drought early warning system (DEWS) would accomplish the drought profiling tasks and fulfill the prerequisites of the long-term goals of DRM philosophy.

There are currently three institutions that map and monitor droughts and issue monthly warnings on food security at global level: the FAO's Global Information and Early Warning System on Food and Agriculture (GIEWS), the Humanitarian Early Warning Service (HEWS) by the World Food Program (WFP) which takes inputs from the Famine Early Warning System NETwork (FEWSNET), and the Benfield Hazard Research Center of the University College London (Grasso 2004). In the context of operational monitoring of famine conditions and food insecurity in the drought prone countries in Africa, there are three institutions namely the USAID-funded FEWSNET, the European Union funded Monitoring Agriculture with Remote Sensing (MARS), the Netherlands based Environmental Analysis & Remote Sensing (EARS) funded food assessment by satellite technology (FAST) service, and the experimental Africa RiskView platform sponsored by the UN WFP.

The U.S. Agency for International Development (USAID) created FEWS NET in mid 1980s with the goal of mitigating the agro-meteorological shocks especially in the food insecure countries of Africa and Latin America. The objectives of the FEWS NET system are three-tiered (Funk and Verdin 2010): vulnerability identification and impact assessment, development of appropriate contingency plans, and design and implementation of timely disaster relief packages. The U.S. Geological Survey (USGS), National Aeronautics and Space Administration (NASA), the National Oceanic and Atmospheric Administration (NOAA) along with

regional experts in FEWS NET countries participate in helping meet these objectives.

FEWS NET monitoring of drought conditions is based on a number of remotely sensed products. Satellite rainfall estimates (RFE2) (Xie and Arkin 1997), which combine satellite thermal infrared measurements with microwave and station data to derive many products such as the SPI, crop, soil moisture and runoff models; and these are hosted on http://earlywarning.usgs.gov/fews/africa/index.php. FEWS NET uses the water requirement satisfaction index (WRSI) as a primary agricultural drought hazard index as a proxy for crop yield. Verdin and Klaver (2002) had demonstrated the use of WRSI algorithm to depict the root zone soil water conditions in a gridded cell-based modeling environment. The gridded WRSI is generated by customized software called Geospatial Water Requirement Satisfaction Index (GeoWRSI) (Magadzire 2009). GeoWRSI uses gridded estimates of satellite rainfall; potential evapotranspiration (PET) (using the Penman-Monteith equation); soil water holding capacity; and crop-specific characteristics such as the length of growing period, and crop coefficients (K_c) (Doorenbos and Pruitt 1977).

The United Nations International Strategy for Disaster Reduction (UNISDR) publishes Global Assessment Report (GAR) addressing all types of disaster risk reduction, including drought. In some of the most drought vulnerable areas of the world there are significant difficulties in getting data to develop risk models, especially from the famine and drought affected countries in Africa. The GAR 2011 reported that in the absence of a credible drought risk model, there is a need to understand agricultural drought impacts and losses using appropriate soil moisture based drought hazard indices.

The UNISDR and the FEWS NET initiated a collaborative study in 2012 to identify and develop a probabilistic agricultural drought risk methodology using satellite estimated rainfall (Phase 1) for GAR13 report. As the emphasis was on agricultural drought risks, following definition of agricultural drought was adopted in the above study: *agricultural drought is characterized by loss in crop production as a result of reduction in crop area and/or lowering of crop yield due to shortage of soil water in its root zone; the loss of crop yield at the end of the season interpreted as a function of the actual crop evapotranspiration deficit relative to its potential evapotranspiration demand*". Standard risk analysis steps – hazard, exposure, and vulnerability were followed; continuous loss exceedance probability (LEP) curves for maize in Rift Valley, Kenya, Malawi and Mozambique, and millets in Niger were generated using the historical and long term synthetic rainfall data for GAR 13 report. A detailed description of the study area, data used; the procedural steps are described in see Appendix A. The risk metrics (average annual loss and other standard return period losses) generated, and corresponding drought frequency maps are published in Harikishan and Husak (2014).

4.   Method and Data used

In view of the increasing evidence of the changing climate, and the importance of assessing its impacts on rainfed crop productivity in drought and famine prone countries of Africa, the scope of the UNISDR-

FEWSNET collaborative study was expanded by expanding its objective to generating LEP curves (for maize in Rift Valley, Kenya, and for millets in Niger in West Sahel) using probabilistic analysis of agricultural drought risks for probable near-future climate scenario (2016_2035) for the GAR15 report (Phase 2).

Following sections highlight different components in phase 2 of this study and results obtained:

4.1   Hazard analysis

The results of the UNISDR-FEWSNET collaborative study on agricultural drought risk analysis in phase 1 used satellite RFE (Harikishan and Husak 2014). The main improvement of hazard analysis in phase 2 of this study has been the use of CHIRPS (Funk et al. 2014) data (in place of satellite RFE). While satellite RFE data (Xie and Arkin 1997) was available from 2001 onwards, CHIRPS data is available from 1981 onwards are available till present date. This enlarged satellite estimated rainfall data set has become an invaluable input in the present study.

CHIRPS (Climate Hazards group InfraRed Precipitation with Stations) precipitation grids (50°S–50°N, 180°E–180°W at 0.05° at 5– and 10-day intervals) are generated by the U.S. Geological Survey Earth Resources Observation and Science Center in collaboration with University of California, Santa Barbara Climate Hazards Group. The main data sources for generating CHIRPS data are (i) the monthly precipitation grids of climatology describing 5- and 10-day long-term average accumulated rainfall and which represent expected sequences of rainfall at each location for the above periods; (ii) quasi-global geostationary thermal infrared (IR) satellite observations from 2 NOAA sources, the CPC (Climate Prediction Center) 0.5 hour temporal resolution and 4 sq.km spatial resolution data (2000-present), and NCDC (National Climatic Data Center) B1 IR (3 hour temporal resolution and 8 km spatial resolution data for 1981-2000) (iii) the Tropical Rainfall Measuring Mission (TRMM) 3B42 product from NASA; (iv) atmospheric model rainfall fields from the NOAA Climate Forecast System, version 2 (CFSv2); all of which are reinforced by (v) using in situ precipitation observations obtained from a host of ground rain gauge stations and variety of sources including national and regional meteorological services (Funk et al. 2014).

The quasi-global CHIRPS precipitation grids have been generated in the following manner: (i) InfraRed Precipitation (IRP) rainfall estimates (mm) have been generated (from thermal satellites) by converting the percentage of time the cold cloud top temperatures remain below the threshold (<235° K) into millimeters of precipitation (using previously available local TRMM 3B42 precipitation calibrations), (ii) the above rainfall estimates have been normalized by dividing them with corresponding long-term (1981–2012) means, (iii) the percent of normal InfraRed accumulations have been multiplied by the corresponding climatological (average expected normal values) to produce an unbiased gridded estimates, and (iv) the final precipitation grid (CHIRPS) is obtained by blending it with the ground rain gauge network data (Funk et al. 2014).

In the present study, the dekadal CHIRPS data has been used to re-generate the baseline (1981_2010) LEP curves for the GAR15 report. These new LEP curves are more comprehensive as they include more historical drought-event losses that have occurred since 1981 in the study areas. It is important to note that the increased depth of CHIRPS data has a two-fold benefit (i) help in generating more representative long-term synthetic rainfall time series (500 years) for baseline (1981_2010) scenario, and (ii) facilitate improved forecasting of rainfall regime corresponding to 2016_2035 climate scenario.

Rainfall regimes for near-future (2016_2035) scenario

The IPCC AR5 (IPCC 2014) states that the impacts from climate-related extremes viz., heat waves, droughts, floods, and such, highlight significant vulnerability of natural and human ecosystems caused by the changing climate variability. The projected climate warming has been defined under two emission scenarios (low and high) characterized as *representative concentration pathways* (RCPs 2.6 and 8.5) respectively. Further, it is deduced that the risks evolving in near-term (2010-2050) will emanate from the interactions among the changing climate, natural and man-made ecosystems, and socio-economics; with the adaptations influencing the near-term outcomes. Again, it is stated that the second half of the 21st Century (2050-2100) and beyond, will be influenced by global temperature- increase corresponding as per the divergent emission scenarios; with near- and long-term adaptation and mitigation measures, and the development pathways determining the consequent risks.

There are about 24 different GCMs developed by more than a dozen climate research centers around the world in support of the IPCC activities. The corresponding projections have been observed to be markedly different due to different numerical modeling methods, spatial resolutions and sub-grid scale parameters. Villegas and Jarvis (2010) observed that there are different downscaling techniques - smoothing, spatial interpolation, statistical or neural network approaches, applied to coarse resolution GCM (Global Climate Model) outputs (cell size of 300 km) for modeling the climate-impacts on biodiversity, natural and man-made ecosystems, species distributions, landscape planning and such. While each downscaling technique varies in accuracy depending on output resolution, computational ease and robustness, their selection depends on the feasibility of computational processing and storage facilities, topography of land, and availability of ground data to calibrate the models. While spatial downscaling is costly, needs significant computing space and time resources, whereas the statistical downscaling tends to reduce variances and provides smoothed surfaces of probable future climates. Consequently, the multitude of downscaled GCM projections have been observed to generate varied forecasts for future climates; which in turn have resulted in significant scientific discord in the projected impacts of climate change on agriculture and biodiversity (Villegas and Jarvis 2010).

As the present study (phase 2) is focused on forecasting the impacts of changing climate (which falls in the near-term i.e., 2016_2035) on agricultural productivity in Africa, a decadal-to-multidecadal (D2M) approach (Enfield and Serrano 2006) has been adopted to generate

multivariate stochastic climate sequences representing the 2016_2035 rainfall regime using historical climate data (1981_2010) in the above region. Enfield and Serrano (2006) reviewed the literature linking D2M climate variability to circulation patterns in terrestrial oceans and seas: El Nino-Southern Oscillation (ENSO)-like Pacific Decadal Oscillation (PDO); the Interdecadal Pacific Oscillation (IPO); the Arctic Oscillation (AO); the North Atlantic Oscillation (NAO); and the Atlantic Multidecadal Oscillation (AMO); further correlating them to the ecological impacts, natural disasters like floods and droughts in different parts of the earth.

The Climate Hazards Group at University of California, Santa Barbara has noted a strong relationship in March-May (MAM) rainfall in the Greater Horn of Africa and West Sahel to Sea Surface Temperatures (SSTs) in the Indian and Pacific Oceans respectively. The approach used in the present study recognized the strengths of climate models in capturing variability and trends in Sea Surface Temperatures (SSTs), while minimizing the impact of less reliable precipitation forecasts. As a first step, a selection of runs from the Coupled Model Intercomparison Project Phase 5 (CMIP5) were first compared with observed NOAA's Optimum Interpolation SST dataset to see how well the CMIP5 data lined up with the best available estimates. With a confirmation of the CMIP5 ability to capture historic SSTs, the El Nino signal that dominates ocean variability removed from the historical and forecast CMIP5 data, leaving differences in SST. A 20 year composite of the forecast period from 2016-2035 resulting in a mean difference field to represent this period was established. These forecast-difference fields capture less distinct variability in the oceans, and may also negate any trends. The 20 year composite was then compared to the CMIP5 differences from 1981-2013 to find the similarity with each individual year.

The above similarity-approach was used to derive weight for each year, which in turn, was used in a bootstrapping scheme to derive 500 simulations of near-term (2016_2035) future rainfall regimes by sampling from the CHIRPS dataset. These resulting simulations captured the variability and trend resulting from forecast SST data, while retaining spatial correlations inherent in decadal rainfall data. The ensuing long term synthetic rainfall time series corresponding to near-term (2016_2035) future climate scenario has now been used to run using GeoWRSI (Magadzire 2009); the corresponding end-of-season WRSI representing hazard time series for near-term (2016_2035) climate scenario.

4.2   Exposure analysis

The availability of satellite estimated precipitation data from 1981 onwards has enabled the use of crop area/yield statistics (at district resolution) in the selected study areas in this study. Maize area/yield statistics from 2001 to 2012 in Rift Valley, Kenya; from 1984 to 2009 in Malawi; and millets area/yield statistics from 1983 to 2007 in Niger have been used to expand the exposure data base. In addition, the extended data has also facilitated modeling the historical drought-induced maize and millets production losses from mid-80s in the above countries. It is important to note in the extended exposure data that, similar to the observation in the earlier study, the drought impact on crop production

was reflected more prominently in (rainfed) crop yields than in crop areas.

4.3   Vulnerability analysis

Modeling of drought vulnerability functions for the selected crops consisted of developing the relative yield deficit versus relative ET (evapotranspiration) deficit functions (described in Harikishan and Husak 2014) using the extended hazard and exposure data (1981 onwards) for the baseline scenario for the selected crops in the selected study areas in the present study.

Drought vulnerability functions for maize in the Rift Valley province in Kenya and Malawi; and for millets in Niger are depicted in Fig.2 (insets a, b, and c) respectively. It can be observed from Table 1 that the slopes of (yield loss coefficient) K_y for maize among the countries are different, indicating different rates of yield losses due to drought. The average slope of the drought yield-loss function for maize in Kenya and Malawi is about 10% more than that that cited for maize by the FAO (http://www.fao.org/nr/water/cropinfo_maize.html.)

A summary of the drought vulnerability models for each country is presented in Table 1, which list the slope, intercept and r^2 between the modeled relative evapotranspiration deficit and relative yield loss based on the identified drought events.

The tabulated p-value indicates the high degree of significance obtained in the statistical regression between the relative deficits in evapotranspiration and the yields for the staple crops in the selected countries. According to the p-values (Student t-test) listed in Table 1, it can be seen that all the relationships can be considered significant at 5% level.

Table 1: Details of statistical regression between relative-yield deficit with relative evapotranspiration deficit for maize and millets

Country	Crop	Slope	r2	p-value
Rift Valley, Kenya	Maize	1.3505	0.21	0.00040
Malawi	Maize	1.4513	0.50	0.00003
Niger	Millets	1.362	0.53	0.00005

Typically a WRSI less than 0.5 correspond to conditions nearing total crop failure (Senay and Verdin 2002). In the present study, it can be observed from inset (a) in Fig. 2 that the maize drought vulnerability function in Rift Valley, Kenya shows the relative evapotranspiration deficit (1-EOS WRSI) falling below 0.5. This indicates an increased range of WRSI sensitivity to capture maize yield losses especially in drought prone areas. Similar observation is also made for millets from inset (c) in Fig. 2 where WRSI in the millets drought yield vulnerability function goes below 0.5 showing increased sensitivity of WRSI.

Fig.2 Drought vulnerability models for (a) maize in Rift Valley, Kenya, (b) maize in Malawi, and (c) millets in Niger
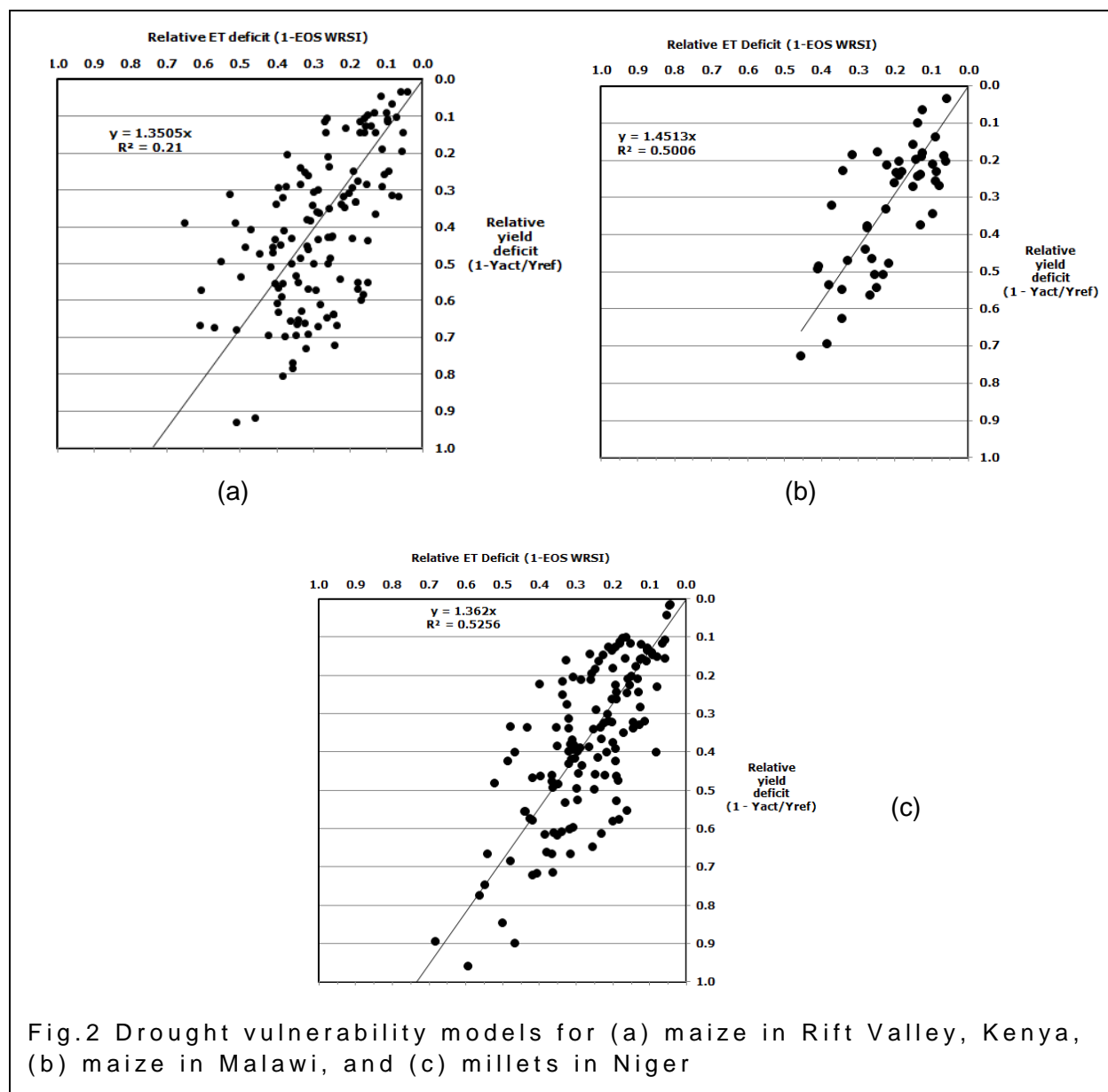
4.4   Risk metrics - LEP curves and return period losses

Loss exceedance probability (LEP) curve is a probabilistic economic or physical loss profile characterizing the response of a country (or a region) to a particular disaster (natural or man-made). It explains the probability that a given magnitude of loss will be exceeded in a given time period. Loss may be expressed either in absolute magnitude (tonnage of crop production lost or local or international currency) or in relative terms (percent of total production or GDP and such).

LEP curve is a continuous probabilistic distribution function of drought-induced losses; and in the present study it has been constructed in two steps – (i) using historical drought events from the loss records available in the country (or region), (ii) and simulated-loss data time series corresponding to synthetic drought events. In addition, standard loss metrics in terms of tonnage losses (production) as well as pin percent of total crop production in the study regions for different return periods (RP) of drought have also been tabulated. The two most commonly used risk metrics are the average annual loss (AAL) and the probable maximum loss (PML). AAL represents the yearly loss averaged over a long period of time while the PML is associated with a 1-in-100 year drought in the context of agricultural drought (Harikishan and Husak 2014).

In this study, LEP curves corresponding to the baseline (1981_2010) and near-term (2016_2035) future climate scenario have been generated in the following steps:

(i)   develop drought vulnerability functions for maize in Rift Valley, Kenya and Malawi; and for millets in Niger using CHIRPS data (Section 4.3)
(ii)   develop national and local level historical drought event losses using the historical exposure data and EOS WRSI corresponding to baseline (1981_2010) hazard data in the study area
(iii)   generate long-term synthetic time series rainfall data (500 years) applying boot strapping algorithms on CHIRPS data
(iv)   run GeowRSI using 500 years of synthetic rainfall time series (based 1981_2010 baseline data) to generate EOS WRSI time series corresponding to above baseline period
(v)   apply historical drought vulnerability functions and generate continuous LEP curve for the (1981_2010) baseline scenario
(vi)   run GeoWRSI using rainfall data corresponding to near-term (2016_2035) climate scenario and generate corresponding drought (EOS WRSI) hazard time series
(vii)   apply historical drought vulnerability functions using hazard time series (EOS WRSI) time series corresponding to near-term (2016_2035) climate scenario
(viii) generate continuous LEP curve corresponding to near-term (2016_2035) climate scenario for the selected crops in the selected study areas
(ix)   generate risk metrics (return period losses and drought frequency maps) for comparative evaluation of agricultural drought risks corresponding to the baseline (1981_2010) and near-term (2016_2035) climate scenarios.

In addition to tabulating AAL and PML, return period losses - losses corresponding to 1-in-10, 1-in-20, 1-in-50 and 1-in-100 year droughts (both in terms of tonnage and percent of total crop production) have also been listed. Average annual loss and drought frequency maps have also been generated from the count (number of times) of drought-incidence in the 500-year simulated time series corresponding to baseline (1981_2010) and near-term (2016_2035) climate scenarios in the present study.

5.   Results and Discussion

LEP curves and risk metrics for maize in Rift Valley, Kenya

Fig. 3 portrays the LEP curves corresponding to historical event losses (1981_2010) (blue dots); simulated LEP curve for baseline (1981_2010) (black line); and simulated LEP curve for near-term (2016_2035) scenario (red line) for maize in Rift Valley, Kenya. The losses have been expressed in terms of metric tonnes. Fig. 4 depicts the above LEP curves (in terms of percent of maize production in 2012) corresponding to the baseline (1981_2010 in black) and near-future (2016_2035 in red) climate scenarios in terms of percentages respectively.

Table 2 lists the province level return period losses corresponding to annual, 1 in 5, 10, 20, 50 and 100 years for maize in Rift valley, Kenya corresponding to baseline (1981_2010) and near-term (2016_2035) climate scenarios in absolute production losses (metric tonnes) and in terms of percent of total maize production during 2012 in Rift Valley, Kenya.

Fig. 3 Loss exceedance probability curves for maize corresponding to baseline (1981_2010) and near-term (2016_2035) climate scenarios in Rift Valley, Kenya (expressed in terms of metric tonnes)
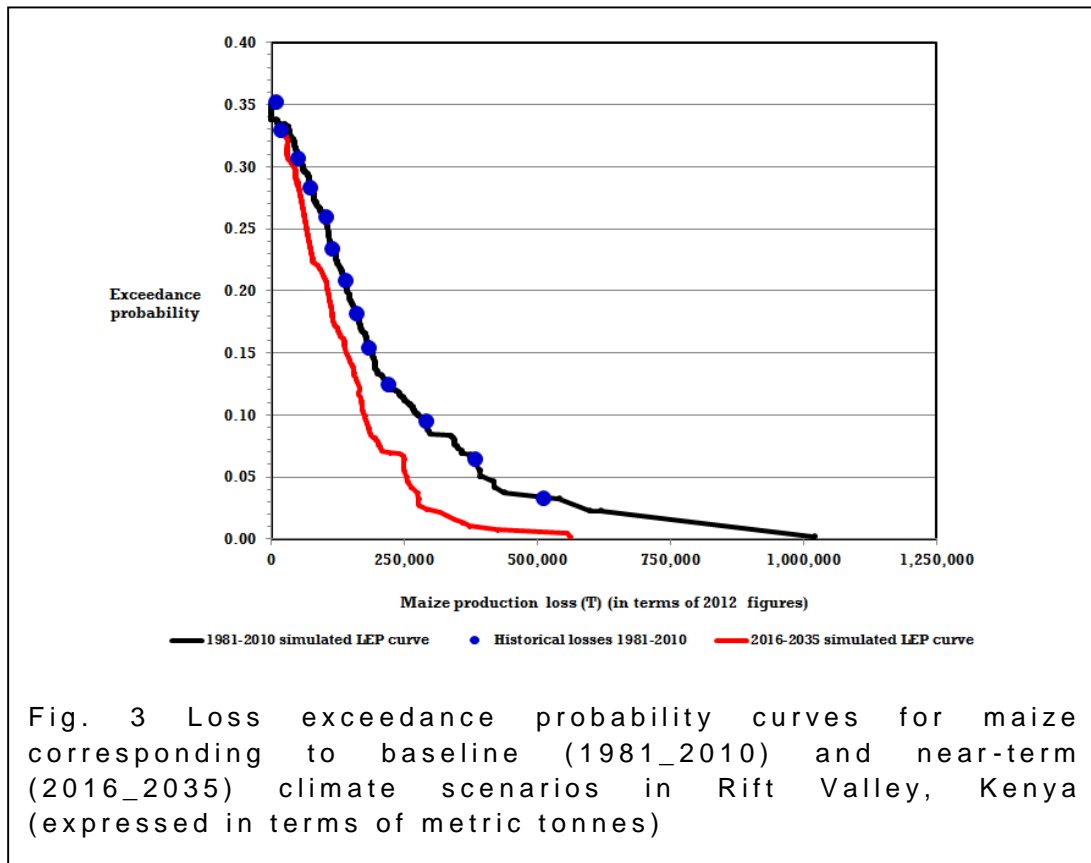
It can be observed from Fig. 3 and 4, and from Table 2, that agricultural drought risk to maize is forecasted to reduce in the near-future (2016_2035). The PML (Probable maximum loss corresponding to 1-in-100 year drought) would reduce from 866,440 T (baseline) to 351,225 T during 2016_2035 (near-future) in Rift Valley, Kenya

Fig. 4 Loss exceedance probability curves for maize corresponding to baseline (1981_2010) and near-term (2016_2035) climate scenarios in Rift Valley, Kenya (expressed as percent of total maize production in above province)
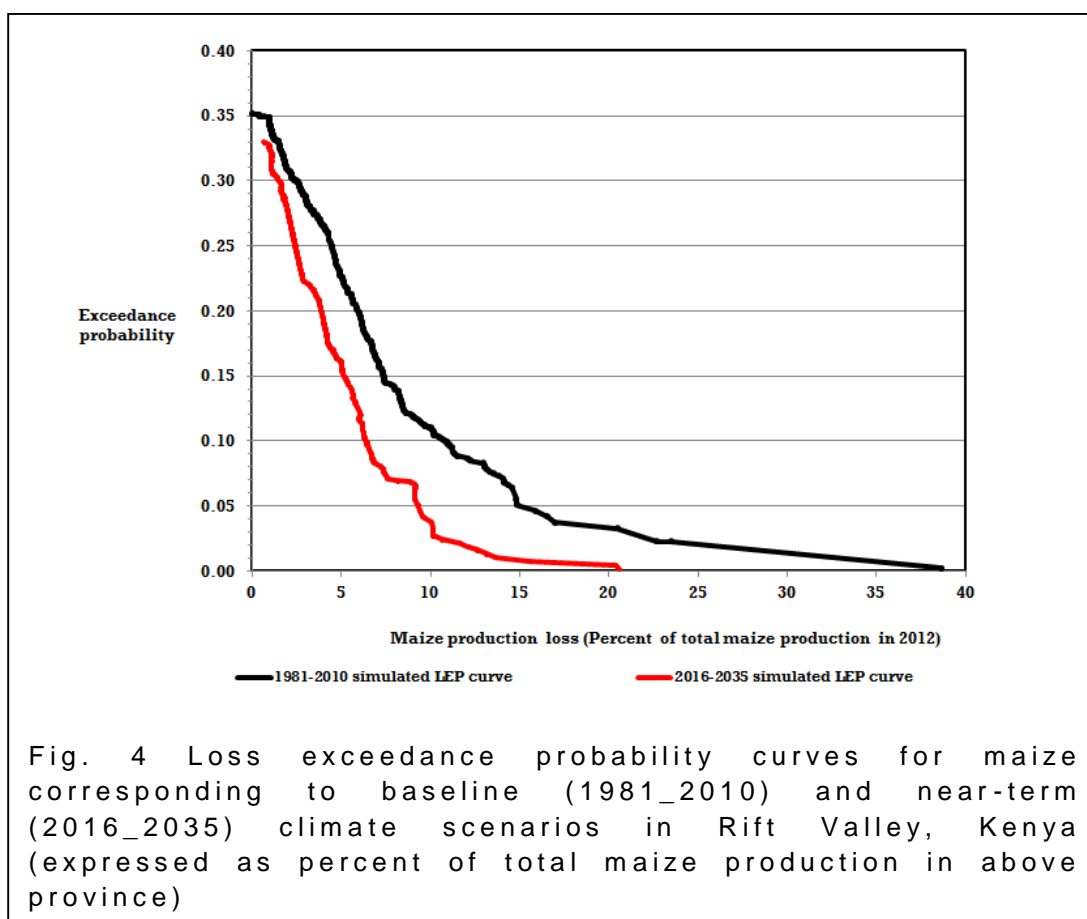
The average annual loss (AAL) is projected to be 48,463 T (1.78% of the total maize production in the Rift Valley Province) while it is 78,190 T (2.86% of the total maize production in Rift Valley Province).

Table 2: Return period losses for maize in Rift Valley, Kenya (Figures in the brackets indicate losses in percent of total maize production in 2012 in the above region)

S.no	Exceedance probability (EP)	Return period (RP)	Baseline losses (1981-2010) (T)	Changing climate (2016-2035) (T)
1	0.01	1 in 100 years	866,440 (31%)	351,225 (13%)
2	0.02	1 in 50 years	674,125 (25%)	333,145 (12%)
3	0.05	1 in 20 years	390,680 (15%)	263,400 (10%)
4	0.10	1 in 10 years	275,125 (10%)	179,400 (7%)
5	0.20	1 in 5 years	141,600 (5%)	113,420 (4%)
6	Average annual loss	AAL	78,190 (3%)	48,463 (2%)

Another significant observation is that the losses corresponding to droughts with shorter return periods are almost similar in the two time horizons, while losses corresponding to longer return periods (>1-in-5 tears) would decrease significantly in the near-future (2016_2035)when compared to the baseline (1981_2010). For example, agricultural drought risk corresponding to a 1-in-5 year drought would only reduce by 1% in the projected near-future. However the losses corresponding to a 1 in 50 year would reduce by 50% i.e., losses in baseline scenario at 25% will reduce to 12% in the near-term 2016_2035 climate scenario).

The positive impact of near-term climate change on maize productivity in Rift Valley, Kenya is explained by comparing the projected dekadal rainfall patterns in the 2016_2035 scenario with the corresponding 1981_2010 rainfall patterns. Fig. 5 depicts the dekadal bar charts in Keiyo and West Pokot districts in Rift Valley Province from 10th dekad (1st to 10th March) to 30th dekad (20th to 31st October).
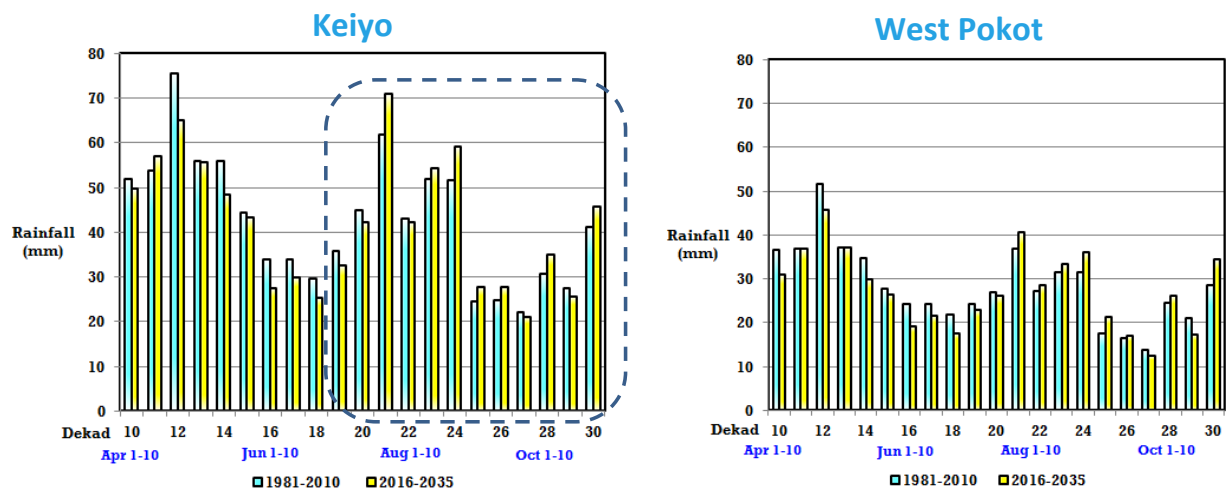

Fig. 5 Dekadal rainfall patterns in Keiyo and West Pokot districts in Rift valley, Kenya, corresponding to baseline (1981_2010) and near-term (2016_2035) climate scenarios

Rainfall patterns in Kenya are governed by the annual migration of the Inter-Tropical Convergence Zone (ITCZ) northwards and southwards of the equator (Rao et al. 2014). Consequently there are two main seasons - wet seasons (March to May) called long rains, and dry seasons (October to December) called short rains respectively. It is seen that the long rains contribute more than 70% to the annual rainfall while the short rains make up the rest. Consequently, there are 2 major cropping seasons in Kenya; the long rains season whose planting begins from mid-March and the season ends in September/mid-October; while planting in the short rains begins in mid-October and the season ends the succeeding February in the Rift Valley, Kenya.

It can be observed from Fig.5 that the dekadal rainfall during the initial part of the growth season (March to May) in the near-term (2016_2035) climate scenario is relatively less compared to that in the baseline (1981_2010) scenario. It can be inferred that the maize cultivation will

be affected in its sowing stages with area being lost due to insufficient rainfall in future. However, this lowered dekadal rainfall exists only till the 18th dekad (end-of-June). In the latter part of the season) from 18th dekad to 30th dekad, increases in the projected dekadal rainfall (2016_2035) compared to baseline (1981_2010) in the study area will enhance the maize productivity in the Rift Valley Province in Kenya. As maize yields are critically dependent on good root zone soil water conditions during the flowering and grain filling periods of maize growth, this projected increased dekadal rainfall during the potential crop yield stages in the future provide evidence for the higher maize yields in the near-term (2016_2035) climate scenario. Consequently, there would be lower agricultural drought frequencies and risks i.e., lower return-period maize production losses and lower AAL.

Rao et al. (2014) based on the DSSAT and APSIM simulations of climate change impacts on principal rainfed crops (maize and groundnut) in selected district in Ethiopia and Kenya, reported a positive impact of climate change on maize productivity. The authors reported that the projected rainfall for the future time horizons indicate increased wetness on either side of the equators; however the projected rainfall decreases with the distance from the equator. The DSSAT and APSIM model projections for maize productivity indicated a 10-30% increase in maize productivity because of the changing climate in the long rains season, while an increase of 50-70% increase is projected in maize productivity in the short rains in the study area. The above study validates the results obtained in the present study.

LEP curves and risk metrics for maize in Malawi

Fig. 6 portrays the LEP curves corresponding to historical event losses (1981_2010) (blue dots); simulated LEP curve for baseline (1981_2010) (black line); and simulated LEP curve for near-term (2016_2035) scenario (red line) for maize in Malawi. The losses have been expressed in terms of metric tonnes. Fig. 7 depicts the above LEP curves (in terms of percent of maize production in 2007) corresponding to the baseline (1981_2010 in black) and near-future (2016_2035 in red) climate scenarios in percentages respectively.

Table 3 lists the country-level return period losses corresponding to annual, 1-in-10, 20, and 50 for maize corresponding to baseline (1981_2010) and near-term (2016_2035) climate scenarios in absolute production losses (metric tonnes) and in terms of percent of total maize production in 2007 in Malawi.

It can be seen from Fig.6 and 7 that there is a negative impact of climate change on maize productivity in Malawi. It can be seen that maize production loss for a 1-in-50 year drought in future climate (2016_2035) is projected to be 441,800 T as compared to 363,800 T estimated for the baseline (1981_2010). It is also observed that in the baseline scenario (1981_2010) Malawi loses about 102,900 T once every 10 years and this loss is going to increase to 159,500 T in the projected near-future (2016_2035) due to climate change. It can be observed from Table 3 that the AAL will increase by about 1.4% (from current baseline scenario at 5% to 6.4%) due to climate change in Malawi.
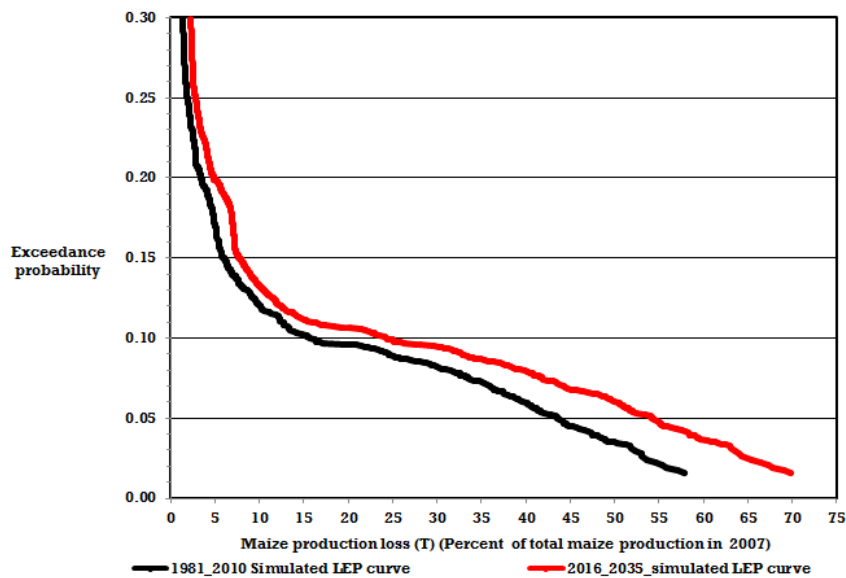
Fig. 6 Loss exceedance probability curves for maize corresponding to baseline (1981_2010) and near-term (2016_2035) climate scenarios in Malawi (expressed in terms of metric tonnes)
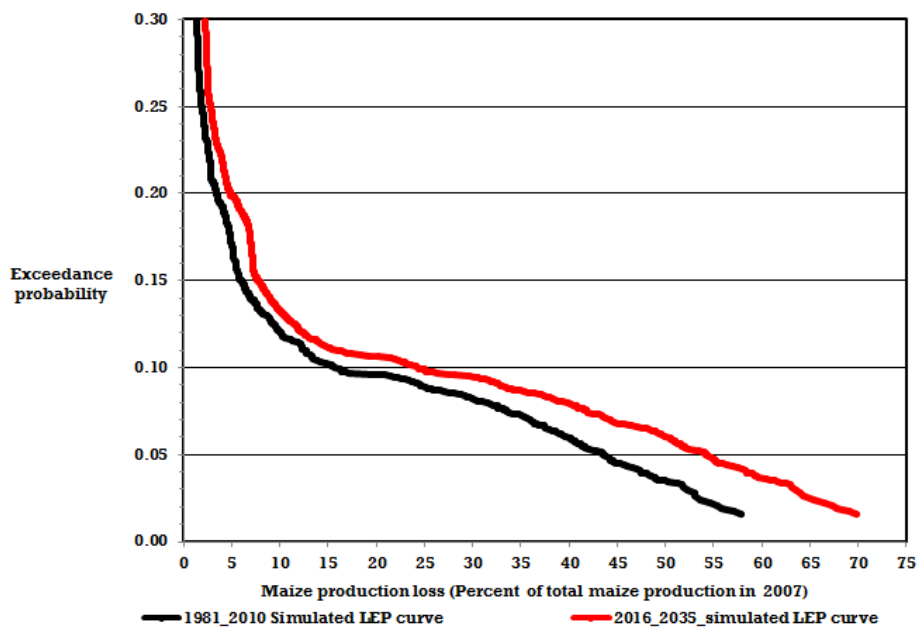

Fig. 7 Loss exceedance probability curves for maize corresponding to baseline (1981_2010) and near-term (2016_2035) climate scenarios in Malawi (expressed as percent of total maize production in Malawi)

Table 3: Return period losses for maize in Malawi (Figures in the brackets indicate losses in percent of total maize production in 2007 in the above region)

S.no	Exceedance probability (EP)	Return period (RP)	Baseline losses (1981-2010) (T)	Changing climate (2016-2035) (T)
1	0.02	1 in 50 years	363,800 (55.4)	441,800 (67.3)
2	0.05	1 in 20 years	285,700 (43.5)	355,700 (54.2)
3	0.10	1 in 10 years	102,900 (15.7)	159,500 (24.3)
4	Average annual loss	AAL	33,115 (5.0)	42,055 (6.4)

.

LEP curves and risk metrics for millets in Niger

Fig. 8 portrays the LEP curves corresponding to historical event losses (1981_2010) (blue dots); simulated LEP curve for baseline (1981_2010) (black line); and simulated LEP curve for near-term (2016_2035) scenario (red line) for millets in Niger. The losses have been expressed in terms of metric tonnes (T). Fig. 9 depicts the above LEP curves (in terms of percent of millet production in 2007) corresponding to the baseline (1981_2010 in black) and near-future (2016_2035 in red) climate scenarios in terms of percentages respectively.

Table 4 lists the country-level return period losses corresponding to annual, 1-in-10, 20, and 50 for millets corresponding to baseline (1981_2010) and near-term (2016_2035) climate scenarios in absolute production losses (metric tonnes) and in terms of percent of total millet production in 2007 in Niger.

Table 4: Return period losses for millets in Niger (Figures in the brackets indicate losses in percent of total millet production in 2007 in the above region)

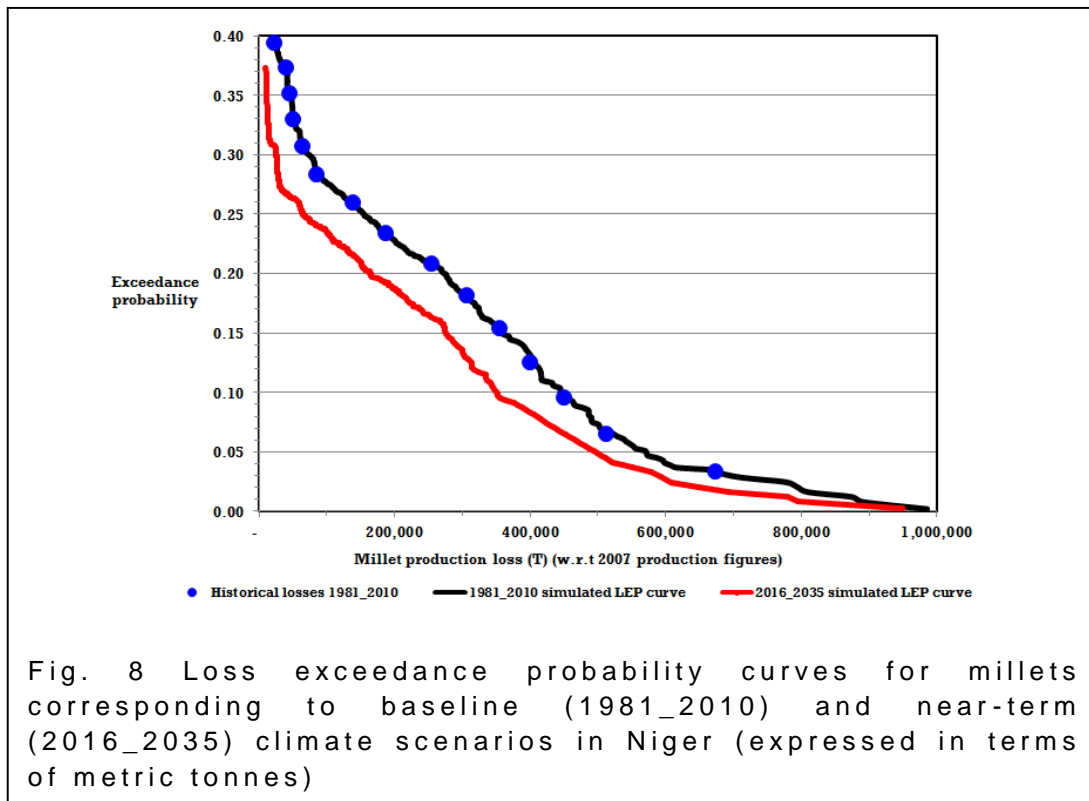| S.no	Exceedance probability (EP)	Return period (RP)	Baseline losses (1981-2010) (T)	Changing climate (2016-2035) (T)
1	0.01	1 in 100 years	880,100 (33%)	785,600 (29%)
2	0.02	1 in 50 years	778,000 (29%)	649,500 (24%)
3	0.05	1 in 20 years	555,750 (21%)	493,200 (18%)
4	0.10	1 in 10 years	443,800 (16.5%)	349,000 (13%)
5	0.20	1 in 5 years	251,650 (9.4%)	163,900 (6%)
6	Average annual loss	AAL	125,700 (4.7%)	88,385 (3.3%)

Fig. 8 Loss exceedance probability curves for millets corresponding to baseline (1981_2010) and near-term (2016_2035) climate scenarios in Niger (expressed in terms of metric tonnes)
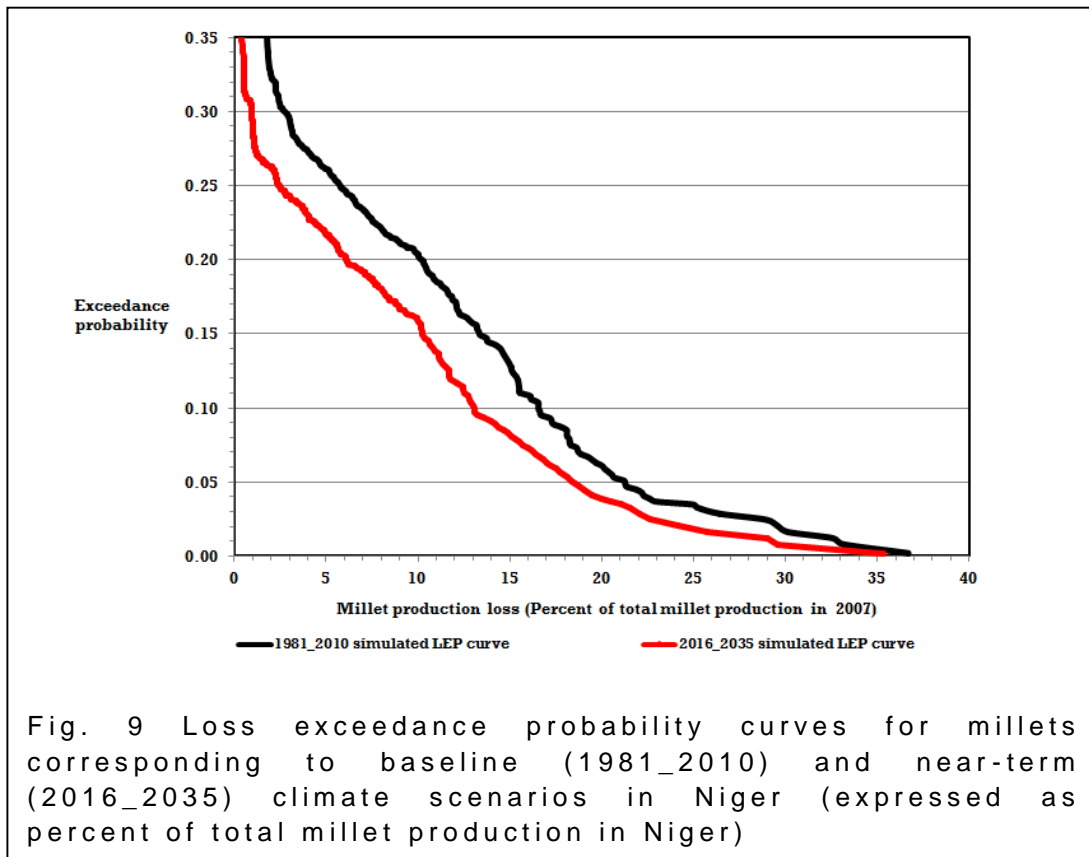

Fig. 9 Loss exceedance probability curves for millets corresponding to baseline (1981_2010) and near-term (2016_2035) climate scenarios in Niger (expressed as percent of total millet production in Niger)

It can be seen from Fig.8 and 9 that there is a positive impact of climate change on millet productivity in Niger. It can be seen that millet production loss for a 1-in-100 year drought in future climate (2016_2035) is projected to be 785,600 T as compared to 880,100 T estimated for the baseline (1981_2010). It is also observed that in the baseline scenario (1981_2010) Niger loses about 251,650 T once every 5 years and this loss is going to decrease to 163,900 T in the projected near-future (2016_2035) due to climate change. In case of millets in Niger the AAL will decrease by about 1.4% (from current baseline scenario at 4.7% to 3.3%) due to climate change.

The positive impact of near-term climate change on millet productivity in Niger is explained by comparing the projected dekadal rainfall patterns in the 2016_2035 scenario with the corresponding 1981_2010 rainfall patterns. Fig. 10 depicts the dekadal bar charts in Dogondoutchi and Madarounfa districts Niger from 16th dekad (1st to 10th June) to 30th dekad (20th to 31st October).
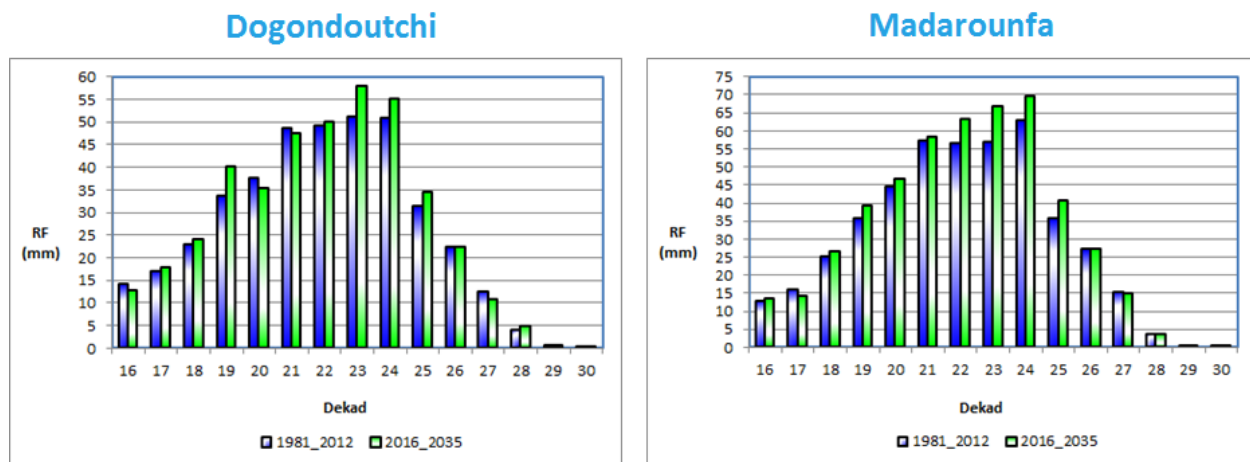

Fig. 10 Dekadal rainfall patterns in Dogondoutchi and Madarounfa districts in Niger corresponding to baseline (1981_2010) and near-term (2016_2035) climate scenarios

In Niger, planting of millet is spread between mid-June and mid-July (18th to 21st dekads) and its harvest occurs from mid-September onwards (Personal Communication, FEWSNET Representative in West Sahel). In relation to the millet cropping calendar, it can be observed from Fig.10 that the dekadal rainfall during (June to September (JJAS) months are consistently higher in the near-term (2016_2035) climate scenario when compared to that in the baseline (1981_2010) scenario; and this relative increase is observed in all the districts in Niger. This projected increase in the rainfall regime in near-future (2016_2035) leads to the positive impact of climate change on millet production in Niger.

Funk et al. (2012) analyzed the historical and changing climate patterns in Niger by conducting rigorous geo-statistical analysis of 110 years of rainfall and temperature records using observations from 209 rain gauges and 12 air temperature stations during the primary crop season-June to September (JJAS). It is reported that decreasing rainfall trends from 50s reversed in md-80s; and these have shown increasing trends till the end of the first decade in the 21st Century. This increasing rainfall trend (in the baseline time frame, 1981_2010) was attributed to the warming of the northern Atlantic Ocean (NAO). The NAO has led to increased temperatures during JJAS months, which in turn, have moved the summer rains further northwards thus increasing rainfall in the above months in the Sahel.

Near term (2016_2035) climate change impacts – Losses in economic terms

This section describes the impacts of the changing climate on rainfed maize and millet productivity in the near-term (2016_2035) in economic terms (% of GDP of the respective countries).

Table 5 lists the climate-change-induced return period losses (PML and AAL) for droughts for maize in the Rift Valley, Kenya and Malawi; and for millets in Niger expressed as percent of corresponding nation's GDP. The economic losses have been referenced to annual producer price of maize and millets in 2007. Again, the PML and AAL have been explained in terms of actual tonnage losses as well as in percent of GDP (2007 figures) corresponding to the Kenya, Malawi and Niger.

Table 5: AAL and PML metrics for maize and millet expressed in USD and percent of GDP corresponding to Kenya, Malawi and Niger respectively.

Country	Crop	Climate scenario	GDP (Constant prices)** Billion USD**	Annual producer price ## USD/MT##	AAL			PML (1 in 100 year)		
					MT	Million USD	% GDP	MT	Million USD	% GDP
Rift Valley, Kenya-2006	Maize	1981_2010	22.504	213.0	78,190	16.7	0.07	866,440	184.6	0.82
		2016_2035			48,463	10.3	0.05	351,225	74.8	0.33
Malawi-2007	Maize	1981_2010	3.458	135.9	33,115	4.5	0.13	363,800	49.4	1.43
		2016_2035			42,055	5.7	0.17	441,800	60.0	1.74
Niger-2007	Millets	1981_2010	4.291	311.3	125,700	39.1	0.91	880,100	274.0	6.38
		2016_2035			88,385	29.3	0.68	785,600	260.3	6.07

** The country-wise GDP (in USD) for the selected crops in the African countries has been extracted from http://data.worldbank.org/

The annual producer prices for the selected crops in the selected years have been extracted from http://faostat3.fao.org/faostat-gateway/go/to/download/P/PP/E

It is seen from Table 5 that the PML for Rift Valley, Kenya decreases from about 1% of the national GDP to 1/3rd (0.33%) in the near-future

due to droughts caused by climate change in this region. However the AAL decreases from 0.07% to 0.03% due to climate change impacts on maize in this Province. On the other hand, the PML increases from 1.43% of Malawian GDP to 1.74% during the 2016_2035 due to climate change impact on maize productivity due to droughts; while the AAL increases marginally from 0.13% to 0.17% in the near-future (2016_2035) due to climate change impact on the above crop. In the case of Niger, the AAL reduces from nearly 1% to 0.68% of GDP (2007 figures) due to climate change impact on millet productivity in the 2016_2035 time horizon. The PML will reduce from about 6.4% to 6.1% of the Niger GDP due to drought-induced changes on millet productivity in the near-term (2016_2035) future climate scenario in Niger.

6.   Summary and Conclusions

Agricultural drought risk profiling, when compared to other risk assessments like floods and cyclones, is a difficult task due to its masked onset, creeping growth, and non-linear vulnerability of rain-fed crops to soil moisture deficits during the crop growing season. While floods and cyclones have well defined zones of vulnerability causing physical damage to crops, agricultural drought damage is more complicated as firstly, its damage is physiological in nature; secondly, its characteristics vary widely in spatio-temporal space; and thirdly, the crop resilience makes it a complex phenomenon to model. In addition to the above, idiosyncratic factors like data-reporting, recording, and re-conciliation habits and practices affect the modeling efforts. There are two major approaches to agricultural drought risk modeling – (i) run a high-frequency high-resolution input based crop process model to monitor the agricultural crop performance, or (ii) conduct an ex-post analysis of the historical drought-induced crop losses to understand the crop response in a given region.

This paper is a follow-up of the Phase 1 of UNISDR-FEWSNET collaborative study on developing and using probabilistic agricultural drought risk assessment for maize in Kenya, Malawi, and Mozambique, and for millets in Niger. The objective in phase 2 of this study was to ascertain drought LEP curves corresponding to the baseline (1981_2010) and near-term (2016_2035) future climate scenario for maize and millets in the above countries. This paper presents the results of phase 2 obtained by using water requirement satisfaction index (WRSI) as the hazard index derived from satellite estimated rainfall (Climate Hazards group InfraRed Precipitation with Stations, CHIRPS). While phase 1 study was accomplished by using satellite RFE data (2001_2010), phase 2 was completed by using CHIRPS data (1981_2010). The backpolated data from 1981 has proven to be a valuable tool for calibrating the maize and millet drought vulnerability models in this study.

Long term synthetic time series of dekadal rainfall has been generated using random boot strapping technique to develop continuous LEP curves for baseline (1981_2010) scenario. A host of GCMs are available, along with downscaling techniques, detailing the anticipated representative concentration pathways (RCPs) and projecting corresponding near- and far-term climate scenarios in the literature. However, towards assessing the impacts of changing climate on maize and millet productivity in near-term (2010_2035) scenario in the selected study areas, the Climate

Hazards Group of University of California, Santa Barbara and FEWSNET adopted a decadal-to-multidecadal (D2M) approach to generate multivariate stochastic climate sequences representing the 2016_2035 rainfall regime in the study areas.

The historical hazard time series (1981_2010) and the actual event losses were first used to construct crop specific drought vulnerability models. The hazard (WRSI) time series corresponding to the synthetic rainfall time series for baseline (1981_2010) and near-term (2016_2035) climate scenarios were converted into synthetic drought event losses. The historical and synthetic drought event losses have been used to generate corresponding representative LEP curves for maize and millet in the study areas. The comparative analysis of the LEP curves and risk metrics (return period losses, PML and AAL) have been tabulated accordingly. Drought frequency maps indicating the drought return intervals at district-level have been generated highlighting the agricultural drought risk characteristics of maize and millet in the respective study areas. The risk metrics have been tabulated in terms of actual tonnage losses; as percent of total crop production; in international monetary units (USD); and as percent of GDP (2007 figures) of the respective countries.

It is important to note that the agricultural drought risks obtained in each study area are restricted (in their interpretations) to that area. For example, the maize drought vulnerability function developed for the Rift Valley Province, Kenya is restricted to that Province alone as it has been derived using the loss data pertaining only to that region; and if the study area is enlarged then the vulnerability function will change, which in turn will affect all subsequent computations using the above function. Further research is necessary to ascertain the agricultural drought risks characteristics in the remaining drought prone provinces in Kenya.

The maize drought LEP curve and the derivatives - risk metrics in Rift Valley Province, Kenya, show a positive impact of climate change on the maize productivity in that Province (this was explained on the basis of seasonal dekadal rainfall distribution in the projected near-term future climate (2016_2035)). Although relatively lower dekadal rainfall till mid-season was projected in the initial dekads (in 2016_2035), however increased rainfall during the latter part of the growing season, especially during the flowering and grain filling stages, are expected to increase the maize productivity (in 2016_2035) in this region. While the maize production losses corresponding to short-return period droughts (up to 1-in-5 years) are observed to be the same for both baseline (1981_2010) and near-term (2016_2035) climate scenarios, however there is a significant decrease in return period maize production losses for larger return periods in this region.

In Malawi, the changing climate (2016_2035) is projected to have a negative impact on maize productivity in Malawi. On the other hand, In Niger, climate change is expected to have a positive impact on millet productivity. Decreases in millet production losses corresponding to different drought return periods as well as PML and AAL in the projected near-future (2016_2035) have been explained using the seasonal dekadal rainfall characteristics in Niger.

The availability and use of hazard and exposure data base from 1981 has enabled to develop more robust drought vulnerability functions in this study. In addition, more robust LEP curves have been generated and the corresponding risk metrics tabulated. It is essential to extend this methodology to other rain-fed crops in the selected countries (and other drought-prone ones as well) in order to establish each country's agricultural drought risk profile for reliable planning, monitoring and evaluation of adaptation measures.

7.   Bibliography

IFPRI (2013). East African Agriculture and Climate Change. A Comprehensive Analysis. IFFPRI Issue brief 76.

Cheng J., Tao J.P. (2010). Fuzzy comprehensive evaluation of drought vulnerability based on analytic hierarchy process. Agriculture and Agricultural Science Procedia. 1:126-135.

Clarke D.J. (2012). Cost-benefit analysis of the African risk capacity facility: Malawi country case study. IFPRI Mimeo.

Doorenbos J., Pruitt W.O. (1977).Crop water requirements. FAO Irrigation and Drainage Paper No 24, FAO, Rome.

Doorenbos J., Kassam A. (1979). Yield Response to Water. FAO Irrigation and Drainage Paper no.33. Rome: FAO.

Enfield, D.B., Serrano, L.C. (2006). Projecting the risk of future Climate Shifts. International Journal of Climatology. 26:885-895. DOI: 10.1002/Joc.1293

Funk C. C., Verdin J.P. (2010). Real-time decision support systems: The famine early warning system network. In: Satellite rainfall applications for surface hydrology. Chapter 17. Gebremichael, M., Hossain, F. (Eds.) Springer Science & Business Media B.V. DOI 10.1007/978-90-481-2915-7_17.

Funk C. C., Rowland J., Alkhalil Adoum, Eilerts G., White L. (2012). A Climate Trend analysis of Niger. Famine Early Warning Systems Network – Information Climate Adaptation Series (http://pubs.usgs.gov/fs/2012/3080/fs2012-3080.pdf).

Funk, C.C., Peterson, P.J., Landsfeld, M.F., Pedreros, D.H., Verdin, J.P., Rowland, J.D., Romero, B.E., Husak, G.J., Michaelsen, J.C., and Verdin, A.P. (2014). A quasi-global precipitation time series for drought monitoring: U.S. Geological Survey Data Series 832, 4 p., *http://dx.doi.org/110.3133/ds832.*

GAR (2011). Drought Risks. Chapter 3. Global Assessment Report on Disaster Risk Reduction. Revealing Risk, Redefining development. United Nations Secretariat of the International Strategy for Disaster Reduction (UNISDR), Geneva, Switzerland.

GAR (2013). Chapter 6: Natural Capital Risk. Global Assessment Report on Disaster Risk Reduction. United Nations Secretariat of the International Strategy for Disaster Reduction (UNISDR), Geneva, Switzerland. Pp.102.

Grasso F. (2004) Early Warning Systems: State-of-Art Analysis and Future Directions, United Nations Environment Program (http://na.unep.net/geas/docs/Early Warning System Report.pdf accessed on 30th September 2011).

Greene, A.M., Hellmuth, M., Lumsden, T. (2012). Stochastic Decadal Climate Simulations for the Berg and Breede Water Management Areas, Western Cape Province, South Africa. Water Resources Research. V48, W06504. Doi:10.1029/2011 WR011152.

Harikishan J., Husak G.J., Funk C., Magadzire T., Adoum Alkhalil, Verdin J.P. (2014). A Probabilistic Approach to Assess Agricultural Drought Risk to Maize in Southern Africa and Millets in Western Sahel using Satellite Estimated Rainfall. International Journal of Disaster Risk Reduction. (In Press). DOI: 10.1016/j.ijdrr.2014.04.002

IPCC (2014). Summary for policymakers. In: Climate Change 2014: Impacts, Adaptation, and Vulnerability. Part A: Global and Sectoral Aspects. Contribution of Working Group II to the Fifth Assessment Report of the Intergovernmental Panel on Climate Change [Field, C.B., V.R. Barros, D.J. Dokken, K.J. Mach, M.D. Mastrandrea, T.E. Bilir, M. Chatterjee, K.L. Ebi, Y.O. Estrada, R.C. Genova, B. Girma, E.S. Kissel, A.N. Levy, S. MacCracken, P.R. Mastrandrea, and L.L. White (eds.)]. Cambridge University Press, Cambridge, United Kingdom and NewYork, NY, USA, pp. 1-32.

Magadzire T. (2009). The Geospatial Water Requirement Satisfaction Index Tool. Technical Manual. USGS Open-File Report. (In Review)

Monnik K. (2000). Role of Drought Early Warning Systems in South Africa's Evolving Drought Policy. In: Wilhite DA, Sivakumar MKV, and Wood DA (Eds.): Early Warning Systems for Drought Preparedness and Drought Management. Proceedings of an Expert Group Meeting in Lisbon, Portugal, 5 - 7 September. WMO, Geneva, Switzerland.

Pauw K., Thurlow J., Van Seventer D. (2010).Droughts and Floods in Malawi. Assessing the Economywide Effects. International Food Policy Research Institute IFPRI) Discussion Paper 00962.

Rao, K.P.C., Sridhar, G., Oyoo, A., Wangui, L. (2014). Assessing the Impacts of Climate Variability and Change on Agricultural Systems in Eastern Africa while Enhancing the Region's Capacity to Undertake Integrated Assessment of Vulnerabilities to Future Changes in Climate. Unpublished Report submitted to Columbia University, Climate Change and African Food Security (CCAFS) (Personal Communication),

Senay G.B., Verdin J. P. (2002). Evaluating the performance of a crop water balance model in estimating regional crop production. Proceedings of the Pecora Symposium 15/Land Satellite Information IV/ISPRS Commission I/FIEOS. Denver CO.

Shi P.J. (2010). Theory and prediction on disaster systems research in a fourth time. Journal of Natural Disaster. V14 (6) 1-7.

Sivakumar M.V.K., Raymond P.M., Wilhite D.A., Wood D.A. (Eds.). (2011). Agricultural Drought Indices. Proceedings of the WMO/UNISDR Expert Group Meeting on Agricultural Drought Indices, 2-4 June 2010, Murcia, Spain: Geneva, Switzerland: World Meteorological Organization. AGM-11, WMO/TD No. 1572; WAOB-2011.

Smith M. (1992). Expert consultation on revision of FAO methodologies for crop water requirements. FAO, Rome, Publication 73.

UNDP (2011). Mainstreaming drought risk management: A primer. Humanitarian requirements for the Horn of Africa Drought. Office for the Coordination of humanitarian Affairs (OCHA) July 2011. United Nations, New York, USA.

UNISDR (2009). Drought Risk Reduction Framework and Practices: Contributing to the Implementation of the Hyogo Framework for Action. United Nations Secretariat of the International Strategy for Disaster Reduction (UNISDR), Geneva, Switzerland.

Verdin J.P., Klaver R. (2002). Grid cell based crop water accounting for the Famine Early Warning System. Hydrological Processes. 16:1617–1630.

Villegas, J.R., Jarvis, A. (2010). Downscaling Global Circulation Model Outputs: The Delta Method. Decision and Policy Analysis. Working Paper No. 1. Agricultura Eco-Efficiente para Reducir la Pobreza. CIAT Publication.

Wilhite D.A., Glantz M.H. (1985). Understanding the drought phenomenon. The role of definitions. *Water International*. 10(3):111-120.

Wilhite D.A. (1991). Drought planning: A process for state government. *Water Resources Bulletin*. 27(1):29-38.

Wilhite D.A., Svoboda M.D. (2000). Drought early warning systems in the context of drought preparedness and mitigation. In: Early warning systems for drought preparedness and drought management. WMO, Geneva, 1-16.

Xie P., Arkin P.A. (1997). Global precipitation: A 17-year monthly analysis based on gauge observations, satellite estimates, and numerical model outputs. Bulletin of American Meteorological Society. 78 (11), 2539-2558.

Appendix A

A.1   Hazard analysis

In this study, the end-of-season WRSI (EOS WRSI) output from the GeoWRSI software (Magadzire 2009) was used as the agricultural drought hazard index. In its simplest form, the EOS WRSI represents the ratio of the seasonal actual crop evapotranspiration to the seasonal crop water requirement (Doorenbos and Kassam 1979). Optimal crop yields are associated with WRSI value of 1 as they represent a situation of 'no water deficit' while a value less than 1 is associated with reduced crop yields. A seasonal WRSI value less than 0.5 was observed as a crop failure condition (Smith 1992).

The actual evapotranspiration (AET) represents the actual soil water extracted by the crop from its root zone. In this regard, GeoWRSI uses the crop coefficients published by FAO for maize (corn), sorghum, millets, wheat, etc. (http://www.fao.org/nr/water/cropinfo_maize.html). Soil water accounting in the crop root zone in GeoWRSI consists of assessing the water supply using satellite estimated rainfall (Magadzire 2009), the pre-existing soil water conditions in the root zone, the crop water demand (satellite estimated PET in conjunction with corresponding

FAO coefficients for maize and millets), and the actual evapotranspiration on a 10-day (dekadal) basis.

The iterative water budgeting exercise in the crop root zone is initiated when the first dekad with more than 25 mm of rain is followed by two dekads with a total rainfall of at least 20 mm. The above criterion signifies the onset of the crop season (start of season or SOS) by filling the crop root zone to its field capacity and ensures most favorable soil moisture conditions for crop emergence. The water budgeting process continues on a dekadal time-interval until the end of the crop phenological cycle as identified by the length of the growing period (LGP). Water budgeting continues through the end-of-season (EOS) which is attained by adding LGP to the SOS at each grid cell. The computational methods used in grid cell soil water accounting, the data used, and the underlying assumptions in GeoWRSI (Magadzire 2009).

This study used the FEWS NET LGP information, provided as part of the GeoWRSI software package, which blends available FAO products with information from field representatives who work closely with national agricultural services in Africa. The GeoWRSI program was run using default settings for field information (length of growing season, crop type, and crop season) and was run over the study areas for the last 10 years (2001−2010). Each dekadal WRSI as well as the EOS WRSI statistics have been spatially averaged over each of the second sub-national districts (18 districts in the Rift Valley province in Kenya; 35 districts in Malawi; 132 districts in Mozambique excluding the urban districts; and 30 Departments in Niger). The resulting statistics generate district and regional WRSI profiles helping to understand the drought incidence and persistence in each location.

A.2   Exposure analysis

Exposure data has been collected from the respective Ministries of Agriculture in Kenya, Malawi, Mozambique and Niger. These data provide an inconsistent record of cropped area and production, because they are not available for many years in the above countries. The maize area and yield statistics are available from 1984 to 2009 in Malawi; from 2000 to 2009 in Mozambique; however, are only available from 2000 to 2006 in Kenya. The millets area and yield statistics are available from 1984 to 2009 in Niger. Mapping these statistics provides spatial context to the tabular data, and gives the user a sense for the major cropping zones within each respective country.

World Bank report stated that there have been 6 major drought events in Malawi during 1982−2008 (Clarke 2012). The economy-wide impacts of extreme hydro-meteorological events on crop production in Malawi and Mozambique are listed in [26]. Adopting an ex-post analytical approach, the crop production losses during the crop seasons of 1986/87, 1991/92, 1993/94, 2003/04 and 2004/05 were analyzed to evaluate the direct and indirect economic losses. The World Bank report observed that the drought impact on crop production in Malawi was reflected more prominently in the rain-fed crop yields than in rain-fed crop areas.

Disasters, in the context of system disaster theory, have been explained (Shi 2005) as consequences of the hazard-formative environmental stability, the hazard risk, and the vulnerability of the exposure. The hazard risk has been expressed as a product of hazard and vulnerability; with hazard of a given magnitude causing more damage to more vulnerable assets-at-risk. There are two broad methodological approaches for agricultural drought vulnerability assessment: the analytic hierarchy process (AHP) and the vulnerability curve method (Pauw et al. 2010).

The analytic hierarchy process (AHP) is a multi-objective decision-making method that delaminates the problem into a multi-layered hierarchical ladder (Cheng and Tao 2010). A matrix consisting of the causative factors is first constructed; appropriate weights are then attributed to the factors at all levels based on field experience and knowledge, and the most representative sequencing is obtained through optimization to model the vulnerability of the system. On the other hand, the vulnerability curve method expresses drought vulnerability as a statistical function between the hazard index and drought-induced reduction in crop production in the study areas. Developing an objective and reliable vulnerability model requires 20−30 years of continuous and error-free crop area and production data[1,2] along with corresponding hazard data, ideally capturing at least six to seven drought events. However, the research presented here is limited to the overlapping period of available crop statistics and the RFE2 database, which limits the present analysis from 2001 to 2009 for Malawi, Mozambique and Niger, and 2001 to 2006 for Kenya.

The modeling of the vulnerability relationships has been based on the FAO guidelines for determining relative yield deficit and relative evapotranspiration deficit (http://www.fao.org/nr/water/cropinfo_maize.html). The steps followed in establishing the vulnerability model are as follows:

- Calculate spatially averaged EOS WRSI statistics for the selected administrative zones.
- Determine the relative evapotranspiration deficit by calculating (1-EOS WRSI).
- Analyze crop production data to determine the drought incidence according to reductions in crop production as identified by corresponding EOS WRSI. This subset of selected years of drought related losses by district are the events used in present drought risk analysis (both for maize and millets).
- Select reference yield ($Y_{reference}$) using the crop yield corresponding to the most temporally proximate season which is neither affected by drought nor flood. The reference yield represents the crop yield obtained in the absence of drought at that location. The yields affected by non-water stress related causes like pests and diseases are ignored in this subset.
- Calculate the relative yield loss ($1-Y_{actual}/Y_{reference}$) corresponding to the identified drought years for the identified events.

- Develop a statistical relationship between the relative yield deficits (maize and millets separately) with the corresponding EOS WRSI for each event.
- Estimate the total drought-induced loss in crop production using the potential crop area in the selected district. Potential crop area is the amount of land likely to be sown in the absence of drought in the region.